Dark Higgs Channel for FERMI GeV γ-ray Excess

P. Ko and Yong Tang

School of Physics,
Korea Institute for Advanced Study,
Seoul 130-722, South Korea

arXiv:1504.03908v2 [hep-ph] 25 Jan 2016

Abstract

Dark Higgs is very generic in dark matter models where DM is stabilized by some spontaneously broken dark gauge symmetries. Motivated by tentative GeV scale γ-ray excess from the galactic center (GC), we investigate a scenario where a pair of dark matter X annihilates into a pair of dark Higgs H_2, which subsequently decays into standard model particles through its mixing with SM Higgs boson. Besides the two-body decay of H_2, we also include multibody decay channels of the dark Higgs. We find that the best-fit point is around $M_X \simeq 95.0$GeV, $M_{H_2} \simeq 86.7$GeV, $\langle\sigma v\rangle \simeq 4.0 \times 10^{-26}\text{cm}^3/\text{s}$ and gives a p-value $\simeq 0.40$. Implication of this result is described in the context of dark matter models with dark gauge symmetries. Since such a dark Higgs boson is very difficult to produce at colliders, indirect DM detections of cosmic γ-rays could be an important probe of dark sectors, complementary to collider searches.

Keywords:

I. INTRODUCTION

Firm evidences for dark matter (DM) come exclusively from the gravitational interaction at the moment. A popular scenario in particle physics models, DM as weakly-interacting massive particles (WIMP), generally predicts that DM should have a mass between $\mathcal{O}(\text{GeV})-\mathcal{O}(\text{TeV})$, with a weak-scale annihilation cross section around $3\times10^{-26}\text{cm}^3/\text{s}$. If those annihilation final states go to standard model particles eventually, there might be notable excesses in cosmic rays and gamma ray searches.

By analyzing *Fermi-LAT*'s public data, several groups [1–11] have been claiming that there might be some excess in the gamma-ray signals from Galactic center [1], inner Galaxy and even some Dwarf Galaxy [13]. The excess is at $E_\gamma \sim O(\text{GeV})$ energy scale and its morphology against the distance to galaxy center is consistent with signals from WIMP DM annihilation, which has motivated intense discussions about DM model-constructions and constraints [14–79]. Besides DM interpretation, astrophysical origins of the excess have also been actively investigated [80–90]. For instance, Refs. [80, 88] showed that gamma-ray emission from unresolved millisecond pulsars is compatible with the excess and can account for at least part of the excess. And Ref. [89, 90] argued that the excess might be comprised entirely of point sources. Recently, `Fermi-LAT` collaboration published a paper [91] on search for DM from Milky Way dwarf spheroidal galaxies and gave stringent constraints. However, since dwarf galaxies might have different DM density profiles from Milky Way halo, such constraints would be relaxed then.

In this paper, we shall exclusively consider DM interpretations. As a first step, it is natural to investigate the GeV excess through annihilation channels that a pair of DM goes to two SM particles directly, such as $q\bar{q}, c\bar{c}, b\bar{b}, t\bar{t}, l^\mp l^\pm, gg, hh, WW, ZZ$ and also their different combinations with some branching fractions. After all, no new particle has been found yet at the LHC, except the Higgs boson. This method has provided valuable information for the favored DM mass and annihilation cross section ranges. Discussions has been extended to cascade two-body decay through new mediators, such as Z' and dark Higgs H_2, which are ubiquitous in new physics beyond SM. In particular, light mediator ($M_{Z',H_2} < 1\text{GeV}$) [56] and heavy $Z^{'}$ [28] cases have been investigated thoroughly.

This work is intended to investigate GeV scale gamma-ray excess in models where DM annihilates into a pair of heavy dark Higgs ($> 1\text{GeV}$) which subsequently could decay into multi-body final states such as WW^* or W^*W^*, where W^* is a virtual W boson. The aim is to provide the ranges of the favored dark Higgs mass, DM mass and the annihilation cross section, which might be useful for particle physics model building, such as hidden sector DM models with local dark gauge symmetries. This work differs from many previous investigation in one essential aspect: we take into account consistently all possible decay modes for heavy dark Higgs, not restricted to its two-body decays.

This paper is organized as follows. In Sec. II, we discuss the theoretical motivation and establish our formalism and notations. In Sec. III, we present our numerical results on the best-fit parameters. Then in Sec. IV, we briefly discuss the implications for DM relic density and constraints from our results. Finally, we give a summary.

[1] Recently, Fermi-LAT also released an paper with some excess [12].

II. FORMALISM

We shall consider the following annihilation channel for self-conjugate DM X,

$$\begin{aligned} X \ + \ X &\to H_2 + H_2, \quad \text{followed by} \\ H_2 \ &\to \ SM + SM(+SM). \end{aligned}$$

Here H_2 denotes the dark Higgs, distinguishing it from the SM-like Higgs H_1 with $M_{H_1} \simeq 125$ GeV. In Ref. [37], the present authors showed that dark Higgs is very generic in dark matter models with dark gauge symmetries, and the GC γ-ray excess can be easily accommodated with the above mechanism (see also Refs. [21, 22, 38] for related works).

H_2 can decay into SM particles through its small mixing with H_1. The mixture between H_2 and H_2 can be easily achieved in particle physics model building.

For example, a real scalar DM X and a complex scalar Φ (dark Higgs that breaks local dark gauge symmetries) can have the following interactions,

$$\mathcal{L} \supset -\lambda_{\phi X} X^2 \Phi^\dagger \Phi - \lambda_{\phi H} \Phi^\dagger \Phi H^\dagger H, \tag{2.1}$$

where H is the SM Higgs doublet. After gauge (or even possible global) symmetry breaking,

$$H \to \left(0, \frac{v_h + h}{\sqrt{2}}\right)^T, \ \phi \to \frac{v_\phi + \phi}{\sqrt{2}}, \tag{2.2}$$

where v_h and v_ϕ are the vacuum expectation values, two neutral scalars h and ϕ will mix with each other through the Higgs portal coupling $\lambda_{\phi H}$, resulting in two mass eigenstates H_1 and H_2 with

$$\begin{pmatrix} H_1 \\ H_2 \end{pmatrix} = \begin{pmatrix} \cos\alpha & -\sin\alpha \\ \sin\alpha & \cos\alpha \end{pmatrix} \begin{pmatrix} h \\ \phi \end{pmatrix}, \tag{2.3}$$

in terms of the mixing angle α.

The above Lagrangian is just one example of many DM models with Higgs portal. One can also consider the case with a real scalar ϕ,

$$\mathcal{L} \supset -\lambda_1 X^2 \phi - \lambda_2 X^2 \phi^2 - \lambda_3 \phi H^\dagger H - \lambda_4 \phi^2 H^\dagger H. \tag{2.4}$$

Again after the electroweak symmetry breaking,

$$H \to \left(0, \frac{v_h + h}{\sqrt{2}}\right)^T, \tag{2.5}$$

h and ϕ are mixed. We can also consider a model with fermionic X with

$$\mathcal{L} \supset -\lambda_1 \bar{X} \gamma_5 X \phi - \lambda_2 \phi H^\dagger H - \lambda_3 \phi^2 H^\dagger H. \tag{2.6}$$

All the above models can easily evade current experimental bounds when α is very small (see discussion in Ref. [92] for example). If one assumes all other possible new particles are heavy, DM X will dominantly annihilate into H_2's.

To be as general as possible, we shall just work with the effective operator, $X^2 H_2^2$ ($\bar{X}\gamma_5 X H_2^2$ for fermionic X), and consider the annihilation process in Fig. 1, assuming that other particles in the dark sector are all heavy enough.

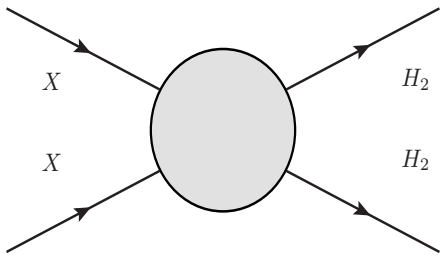

FIG. 1: Feynman diagram due to the effective operator $X^2H_2^2$ ($\bar{X}\gamma_5 X H_2^2$ for fermionic X or $X_\mu X^\mu H_2^2$ for vector X). The actual annihilation process may occur through s or t channel, and contact interaction. Details in the gray bubble depend on various ultraviolet completions. The produced H_2s can have two-, three- or even four-body decay channels.

The produced H_2's could be either relativistic or non-relativistic for $M_{H_2} \ll M_X$ or $M_{H_2} \simeq M_X$, respectively. Different kinematics might lead to significant differences in the gamma-ray spectra. Moreover, depending on the mass of H_2, M_{H_2}, H_2 can dominantly decay into 2 or 3 standard model particles. In our numerical calculation, we use `PYTHIA-6.4` [93] to simulate and tabulate dN_γ^f/dE_γ for the interesting ranges of M_X and M_{H_2}. In particular, we focus on $M_X \geq 5$ GeV and $M_{H_2} \geq 1$ GeV.

The general differential flux of the gamma-ray from the annihilation of self-conjugate DM is given by

$$\frac{d^2\Phi}{dE_\gamma d\Omega} = \frac{1}{8\pi}\sum_f \frac{\langle\sigma v\rangle_{\rm ann}^f}{M_{\rm DM}^2}\frac{dN_\gamma^f}{dE_\gamma}\int_0^\infty dr\rho^2\left(r'\left(r,\theta\right)\right), \tag{2.7}$$

where $\langle\sigma v\rangle_{\rm ann}^f$ is the velocity-averaged annihilation cross section for the annihilation channel f, dN_γ^f/dE_γ is prompt gamma-ray spectrum, $r' = \sqrt{r_\odot^2 + r^2 - 2r_\odot r\cos\theta}$, r is the distance to earth from the DM annihilation point, $r_\odot \simeq 8.5$kpc for solar system and θ is the observation angle between the line-of-sight and the center of Milky Way. An extra factor $1/2$ needs to be included for non-self-conjugate DM, such as complex scalars or Dirac fermions. In our considered case, we have only one annihilation channel, $X + X \to H_2 + H_2$.

For DM density distribution, we use the following generalized NFW profile [94],

$$\rho\left(r\right) = \rho_\odot\left[\frac{r_\odot}{r}\right]^\gamma\left[\frac{1+r_\odot/r_c}{1+r/r_c}\right]^{3-\gamma}, \tag{2.8}$$

with parameters $r_c \simeq 20$kpc and $\rho_\odot \simeq 0.4$GeV/cm^3. We shall adopt the index $\gamma = 1.26$ if not stated otherwise.

III. NUMERICAL ANALYSIS

We first show three cases for the gamma-ray spectrum in Fig. 2. The vertical axis marks the conventional

$$E^2\frac{dN}{dE} \equiv E_\gamma^2\frac{1}{\Delta\Omega}\int_{\Delta\Omega}\frac{d^2\Phi}{dE_\gamma d\Omega}, \tag{3.1}$$

where $\Delta\Omega$ indicates the region of interest. The 24 data points we used to compare with are from Ref. [11], denoted as CCW hereafter.

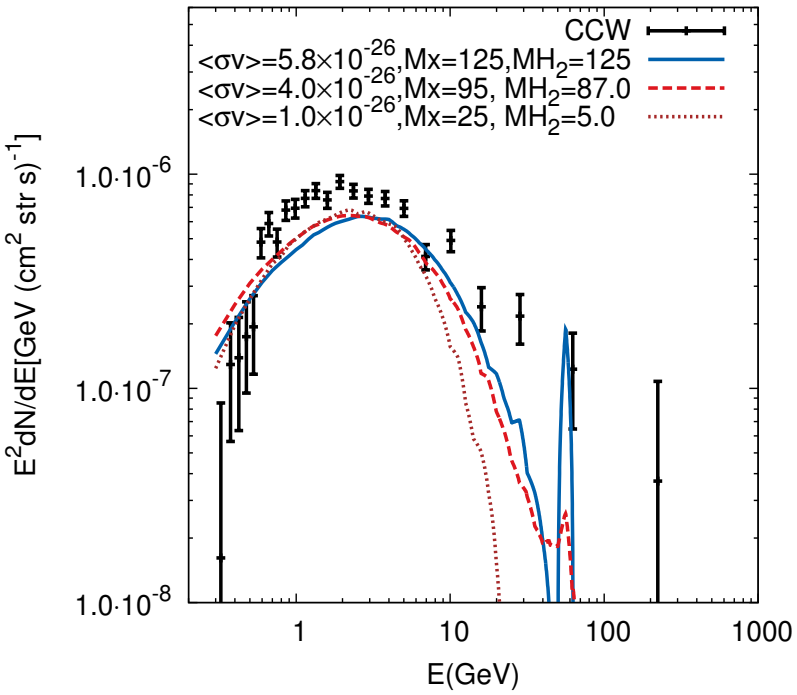

FIG. 2: Three illustrative cases for gamma-ray spectra in contrast with CCW data points [11]. All masses are in GeV unit and σv with cm^3/s. Line shape around $E \simeq M_{H_2}/2$ is due to decay modes, $H_2 \to \gamma\gamma, Z\gamma$.

As we can see, different parameter sets can give different spectrum shape, especially in the high energy regime. When the branching ratios of $H_2 \to \gamma\gamma, Z\gamma$ are increasing, we can see the gamma lines more easily around $E \simeq M_{H_2}/2$. Since the annihilation cross section is at order of $10^{-26}\mathrm{cm}^3/\mathrm{s}$ and the branching ratios of $H_2 \to \gamma\gamma, Z\gamma$ are around 0.2% at most, the considered parameters are still consistent with constraint from gamma-line searches.

We now use the χ^2 function and find its minimum to find out the best fit:

$$\chi^2\left(M_X, M_{H_2}, \langle\sigma v\rangle\right) = \sum_{i,j} \left(\mu_i - f_i\right) \Sigma_{ij}^{-1} \left(\mu_j - f_j\right), \tag{3.2}$$

where μ_i and f_i are the predicted and measured fluxes in the i-th energy bin respectively, and Σ is the 24×24 covariance matrix. We take the numerical values for f_i and Σ from CCW [11]. Minimizing the χ^2 against f_i with respect to M_X, M_{H_2} and $\langle\sigma v\rangle$ gives the best-fit points, and then two-dimensional 1σ, 2σ and 3σ contours are defined at $\Delta\chi^2 \equiv \chi^2 - \chi^2_{\mathrm{min}} = 2.3$, 6.2 and 11.8, respectively.

Fig. 3 is our main result. In the left panel, M_X, M_{H_2} and $\langle\sigma v\rangle$ are freely varied, so that the total degree of freedom (d.o.f.) is 21. The red dot represents the best-fit point with

$$M_X \simeq 95.0\mathrm{GeV},\ M_{H_2} \simeq 86.7\mathrm{GeV},\ \langle\sigma v\rangle \simeq 4.0\times10^{-26}\mathrm{cm}^3/\mathrm{s}, \tag{3.3}$$

gives $\chi^2_{\mathrm{min}} \simeq 22.0$, with the corresponding p-value equal to 0.40.

We also notice that there are two separate regimes, one in the low mass region and the other in high mass region. The higher mass region is basically aligned with $M_{H_2} \simeq M_X$ since otherwise a highly-boosted H_2 would give a harder gamma-ray spectrum. In this region,

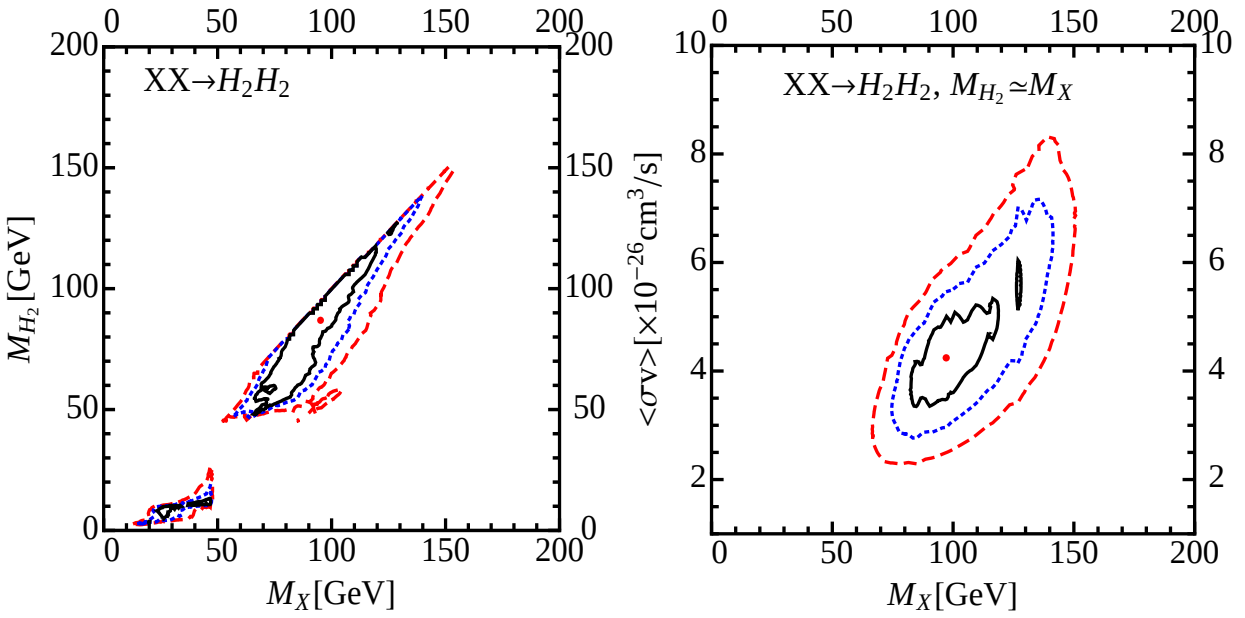

FIG. 3: The regions inside solid(black), dashed(blue) and long-dashed(red) contours correspond to 1σ, 2σ and 3σ, respectively. The red dots inside 1σ contours are the best-fit points. In the left panel, we vary freely M_X, M_{H_2} and $\langle\sigma v\rangle$. While in the right panel, we fix the mass of H_2, $M_{H_2} \simeq M_X$.

H_2 mostly decays into $b\bar{b}$. As one increases the mass of H_2, $H_2 \to W^{\pm}l^{\mp}\nu$, $H_2 \to Zl^{\pm}l^{\mp}$, $H_2 \to \gamma\gamma$ and $H_2 \to \gamma Z$ become more and more important, and all of them give harder gamma-ray spectra either due to the leptonic final states or the gamma lines. Eventually, χ^2 increases significantly when $M_{H_2} \geq 150$GeV.

In the low mass region, the contours are scattered but centered around $M_{H_2} \simeq 10$GeV and such a light H_2 most likely decays into $b\bar{b}, c\bar{c}$ and $\tau^+\tau^-$. Since $c\bar{c}$ and $\tau^+\tau^-$ would give harder spectra than $b\bar{b}$ does, we would need a lower M_X to fit the data, which is exactly what we see in Fig. 2 (dotted curve). Increasing the branching ratios of $c\bar{c}$ and $\tau^+\tau^-$ would require a even lower M_X.

In the right panel, we show a special case in which $M_{H_2} \simeq M_X$, so that the produced H_2s are non-relativistic. In such a case, the d.o.f. is now 22. The best-fit parameters are

$$M_X \simeq M_{H_2} \simeq 97.1\text{GeV}, \ \langle\sigma v\rangle \simeq 4.2 \times 10^{-26}\text{cm}^3/\text{s}, \tag{3.4}$$

which gives $\chi^2_{\text{min}} \simeq 22.5$ and the p-value equal to 0.43. An interesting thing is that $M_X \simeq M_{H_2} \simeq 125$GeV also give a good-fit. This point is equivalent to the channel that DM X annihilates into SM Higgs, which has been already found in previous study [50, 55].

In the left panel of Fig. 4, we fix the mass of dark Higgs to the best-point value, $M_{H_2} = 86.7$, and vary M_X and $\langle\sigma v\rangle$. We show 1σ, 2σ and 3σ contours in terms of solid(black), dashed(blue) and long-dashed(red) curves, respectively. To compare with $b\bar{b}$ channel, we also present 3σ region in the right panel of Fig. 4. The best-fit point is around

$$M_X \simeq 49.4\text{GeV}, \ \langle\sigma v\rangle \simeq 1.75 \times 10^{-26}\text{cm}^3/\text{s}, \tag{3.5}$$

which gives $\chi^2_{\text{min}} \simeq 24.4$ and a p-value, 0.34.

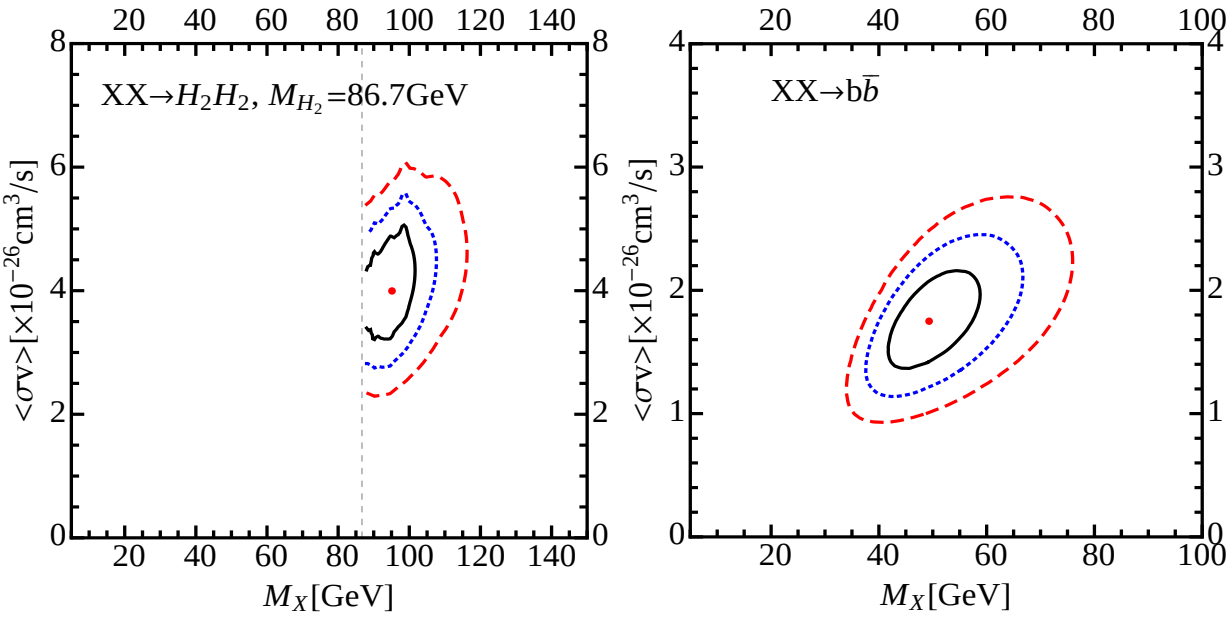

FIG. 4: Regions inside solid(black), dashed(blue) and long-dashed(red) contours correspond to 1σ, 2σ and 3σ, respectively. The red dots inside 1σ contours are the best-fit points. In the left panel, we fix $M_{H_2} = 86.7$GeV, but vary freely M_X and $\langle\sigma v\rangle$. For comparison, in the right panel we consider $XX \to b\bar{b}$ channel.

Channels	Best-fit parameters	$\chi^2_{\rm min}$/d.o.f.	p-value
$XX \to H_2H_2$ (with $M_{H_2} \neq M_X$)	$M_X \simeq 95.0$GeV, $M_{H_2} \simeq 86.7$GeV $\langle\sigma v\rangle \simeq 4.0 \times 10^{-26}$cm^3/s	22.0/21	0.40
$XX \to H_2H_2$ (with $M_{H_2} = M_X$)	$M_X \simeq 97.1$GeV $\langle\sigma v\rangle \simeq 4.2 \times 10^{-26}$cm^3/s	22.5/22	0.43
$XX \to H_1H_1$ (with $M_{H_1} = 125$GeV)	$M_X \simeq 125$GeV $\langle\sigma v\rangle \simeq 5.5 \times 10^{-26}$cm^3/s	24.8/22	0.30
$XX \to b\bar{b}$	$M_X \simeq 49.4$GeV $\langle\sigma v\rangle \simeq 1.75 \times 10^{-26}$cm^3/s	24.4/22	0.34

TABLE I: Summary table for the best fits with three different assumptions.

For completeness and comparison, we also show similar plots in Fig. 5 based on the analysis of Inner Galaxy from Ref. [10]. All parameters are the same as previous except $\gamma = 1.18$ for the DM profile as used Ref. [10]. As shown in Fig. 5, the regions inside contours are much smaller than those in Figs. 3 and 4. This is due to the fact that uncertainties in Ref. [10] are purely statistical. All the best-fit points give $\chi^2 \sim 44$, and the minimal χ^2 is reached when $M_X \simeq 87.0$GeV, $M_{H_2} \simeq 82.1$GeV and $\langle\sigma v\rangle \simeq 4.7 \times 10^{-26}$cm^3/s with $\chi^2_{\rm min}$/d.o.f $\simeq 42.6/(22-3)$ which corresponds to a p-value, 1.5×10^{-3}. It seems that this is not a good fit. However, according to Ref. [10], any value of $\chi^2 \lesssim 50$ should be taken as a reasonable "good fit", given the large systematic uncertainties associated with the background templates choice. Nevertheless, we can easily see that the favored regions are consistent with those in Figs. 3 and 4 within 2-3σ.

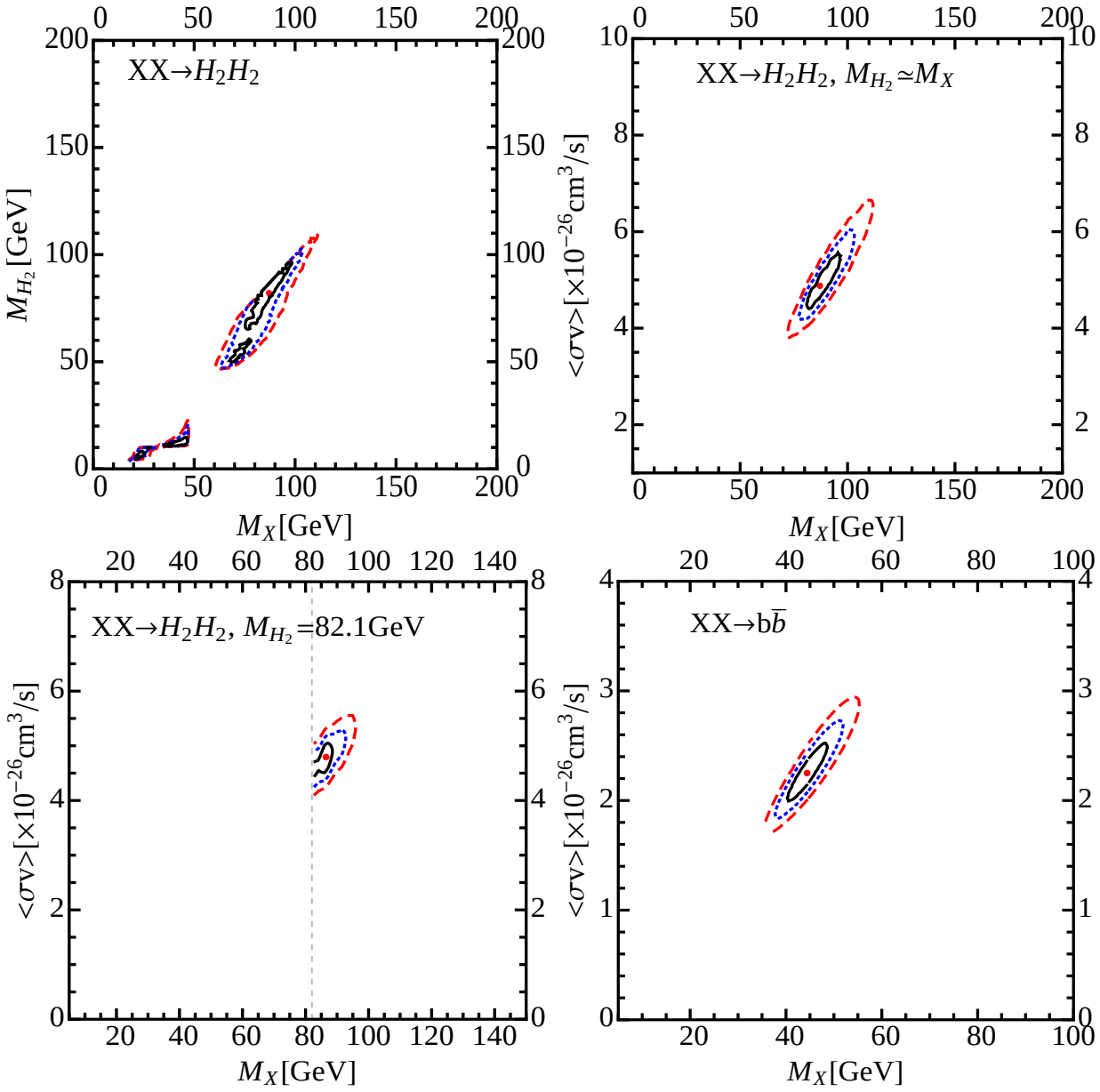

FIG. 5: Similar plots as Figs. 3 and 4, based on results from Ref. [10]. Regions inside solid(black), dashed(blue) and long-dashed(red) contours correspond to 1σ, 2σ and 3σ, respectively. The red dots inside 1σ contours are the best-fit points.

IV. RELIC ABUNDANCE AND PHENOMENOLOGY

So far, we have not discussed any actual concrete DM models, how the correct relic abundance can be achieved and how one can test or constrain this scenario further. Generally, such topics are highly model dependent and the conclusions would differ significantly from one case to another. Still, we can give some general implications from the results obtained earlier in this letter.

From Eqs. (3.3) and (3.4), we notice that the best-fit annihilation cross section for dark Higgs channel is bigger than the canonical value for thermal DM X, $2 \sim 3 \times 10^{-26}\text{cm}^3/\text{s}$,

although still consistent within 2-3σ range. Larger $\langle\sigma v\rangle$ would mean a smaller relic abundance for X. However, the correct relic density can still be reached if we extend the above minimal DM model setup. For example, we may introduce another heavy DM component Y and the total energy fraction of $\Omega_Y + \Omega_X$ is just the observed $\Omega_{\rm DM}$. Suppose Y froze out in the early universe but had decayed into X pairs with a lifetime shorter than the age of Universe. This can be easily achieved if we introduce the following interactions:

$$\delta\mathcal{L} = y_1 Y^2 X^2 + y_2 M_X Y X^2.$$

When y_2 is small enough, say less than 10^{-12}, Y would decay into X pair after BBN epoch or the freeze-out of X's. Before its decay, Y's relic abundance was determined by y_1 through the efficient annihilation process, $Y + Y \to X + X$. Although y_2 is small, it is still technically natural or natural by 't Hooft's naturalness argument because if y_2 is zero, we have an additional Z_2 symmetry for particle Y.

For $b\bar{b}$ channel, the best-fit cross section, Eq. (3.5), is a little smaller than the canonical value. This is not a problem at this stage since the right panel of Fig. 4 shows that canonical value of thermal cross section is within 1-2σ range. Even if it is a problem, we can still imagine that in some concrete models, there could exist some other annihilation channels whose cross sections have velocity dependence or p-wave suppression, $\langle\sigma v\rangle \propto v^2$. For instance, if fermionic DM X has interaction, $\bar{X}X\phi^2$, then $X + \bar{X} \to 2\phi$ is much more suppressed nowadays than at the freeze-out time. Then the sum of cross sections to $\phi\phi$ and $b\bar{b}$ has a canonical value at the freeze-out time but only $b\bar{b}$ channel is important now for its indirect detections.

Here we briefly discuss the related possible particle phenomenology in an explicit UV complete model. We shall note phenomenology is highly model-dependent and we refer to our previous works [21, 37, 38, 92] for some detailed examples. Our discussion here is just focused on the following Lagrangian with $U_X(1)$ gauge symmetry:

$$\begin{aligned}\mathcal{L} \;=\; & \mathcal{L}_{\rm SM} - \frac{1}{4}X_{\mu\nu}X^{\mu\nu} + (D_\mu\Phi)^\dagger(D^\mu\Phi) - \lambda_\Phi\left(\Phi^\dagger\Phi - v_\Phi^2/2\right)^2 \\ & -\lambda_{\Phi H}\left(\Phi^\dagger\Phi - v_\Phi^2/2\right)\left(H^\dagger H - v_H^2/2\right)\;, \end{aligned} \tag{4.1}$$

where in the SM Lagrangian the Higgs potential term is $\lambda_H\left(H^\dagger H - v_H^2/2\right)^2$ and the covariant derivative is defined as $D_\mu\Phi = (\partial_\mu - ig_X X_\mu)\Phi$.

A nonzero vacuum expectation value v_Φ breaks $U(1)_X$ spontaneously. Afterwards, X_μ gets mass $M_X = g_X v_\Phi$ and the dark Higgs field ϕ will mix with the SM Higgs field h through the Higgs portal term, resulting in two mass eigenstates, H_1 and H_2. The mixing angle α in the matrix Eq. (2.3) is determined by

$$\sin 2\alpha = \frac{2\lambda_{H\Phi} v_H v_\Phi}{m_{H_2}^2 - m_{H_1}^2}. \tag{4.2}$$

In this model, gauge boson X_μ is the dark matter because its only couplings, $X_\mu X^\mu H_{1,2}^2$ and $X_\mu X^\mu H_{1,2}$, have accidental Z_2 symmetry which ensure the stability.

The mixing angle is constrained by Higgs signal strength and invisible decay at the LHC [104, 105],

$$\sin^2\alpha \lesssim 0.2, \text{ and } \lambda_{H\Phi} \lesssim 10^{-2} \text{ for } M_{H_2} < 62.5\text{GeV}.$$

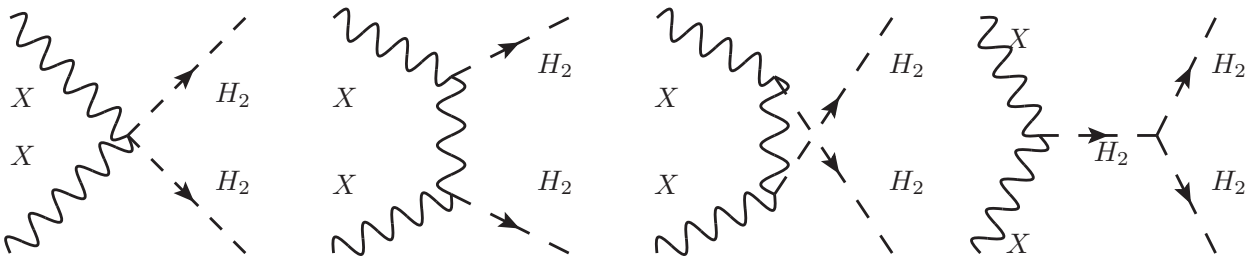

FIG. 6: Feynman diagrams. The last one can be neglected for small λ_Φ.

Due to the allowed small mixing, the dominant annihilation processes for small scalar self-coupling are shown in Fig. 6, their thermal cross section $\langle\sigma v\rangle$ to determine the relic density is given by

$$\langle\sigma v\rangle = \frac{g_X^4\cos^4\alpha}{144\pi M_X^2}\left[3 - \frac{8\left(M_{H_2}^2 - 4M_X^2\right)}{M_{H_2}^2 - 2M_X^2} + \frac{16\left(M_{H_2}^4 - 4M_{H_2}^2M_X^2 + 6M_X^4\right)}{\left(M_{H_2}^2 - 2M_X^2\right)^2}\right]. \tag{4.3}$$

For the above formula, we can determine the required gauge coupling g_X for correct DM density. For instance, if $M_{H_2} \ll M_X$, $\langle\sigma v\rangle \sim 3\times10^{-26}\mathrm{cm}^3/\mathrm{s}$ gives

$$g_X \sim \frac{0.2}{\cos\alpha}\left(\frac{M_X}{100\mathrm{GeV}}\right)^{1/2}.$$

While if $M_{H_2} \simeq M_X$, $\langle\sigma v\rangle \sim 3\times10^{-26}\mathrm{cm}^3/\mathrm{s}$ would give

$$g_X \sim \frac{0.24}{\cos\alpha}\left(\frac{M_X}{100\mathrm{GeV}}\right)^{1/2}.$$

The scalar mixing also lead to possible signal for direct detection of DM. The spin-independent scattering cross section for exchanging scalar mediators is calculated as

$$\begin{aligned}\sigma_p^{\mathrm{SI}} &= \frac{g_X^2 m_p^2 f_p^2\sin^2 2\alpha}{4\pi v_H^2}\left(\frac{1}{M_{H_1}^2} - \frac{1}{M_{H_2}^2}\right)^2, \\ &\simeq 2.2\times10^{-45}\mathrm{cm}^2\left(\frac{g_X s_\alpha c_\alpha}{10^{-2}}\right)^2\left(\frac{75\mathrm{GeV}}{M_{H_2}}\right)^4\left(1 - \frac{M_{H_2}^2}{M_{H_1}^2}\right)^2,\end{aligned} \tag{4.4}$$

which can easily satisfy LUX [106] limit for small mixing angle $\sin\alpha \lesssim 0.05$. This also means that direct detection can place a much stronger limit on $\sin\alpha$ for light dark higgs. Since the production cross section of this second higgs goes like $\sin^2\alpha$, it would be very challenge for probe it at the LHC.

V. SUMMARY

In the letter, we have explored a possibility that the GeV scale γ-ray excess from the galactic center is due to DM pair annihilation into a pair of dark Higgs, followed by the dark

Higgs decay into the SM particles through its small mixing with the SM Higgs boson. Including the correlations among different parameters and varying M_X and M_{H_2} independently, we find that the best fit is obtained if

$$M_X \simeq 95.0\text{GeV}, \quad M_{H_2} \simeq 86.7\text{GeV}, \quad \langle \sigma v \rangle \simeq 4.0 \times 10^{-26}\text{cm}^3/\text{s}$$

If we impose $M_X \simeq M_{H_2}$, we get a similar result (see Table I). This information could be important inputs in dark matter models with dark Higgs boson.

At this stage we cannot make any strong statement about the existence of dark Higgs with mass close to the DM mass $\sim$ 95GeV. However dark Higgs is very generic in DM models where DM is stabilized by some spontaneously broken local (or even global) dark gauge symmetries [21, 22, 37, 64, 95–103]. Since the dark Higgs boson is a SM singlet scalar, it is very difficult to find it at colliders although there are some interesting constraints from the LHC data on the SM Higgs signal strengths [104]. It is simply more difficult to produce them at colliders when the mixing angle is small. It is very amusing to notice that indirect DM detection experiments can be more sensitive to such a dark Higgs than the collider experiments. Compared with more popular dark photon scenario, it is more natural to have flavor dependent couplings of dark Higgs boson to the SM fermions, since its couplings are basically the same as those of the SM Higgs boson modulo the mixing angle effect. This fact makes much easier DM model building [21, 22]. It remains to be seen whether this fit survives in the future data sets, and if there would be any indication of such a dark Higgs from the future collider experiments.

Acknowledgments

We are grateful to C. Weniger for sharing the covariant matrix and an example script. We thank the KIAS Center for Advanced Computation for providing computing resources. YT thanks Xiaodong Li for helpful discussions. This work is supported in part by National Research Foundation of Korea (NRF) Research Grant 2012R1A2A1A01006053, and by the NRF grant funded by the Korea government (MSIP) (No. 2009-0083526) through Korea Neutrino Research Center at Seoul National University (PK).

[1] L. Goodenough and D. Hooper, arXiv:0910.2998 [hep-ph].
[2] D. Hooper and L. Goodenough, Phys. Lett. B **697**, 412 (2011) [arXiv:1010.2752 [hep-ph]].
[3] A. Boyarsky, D. Malyshev and O. Ruchayskiy, Phys. Lett. B **705**, 165 (2011) [arXiv:1012.5839 [hep-ph]].
[4] D. Hooper and T. Linden, Phys. Rev. D **84**, 123005 (2011) [arXiv:1110.0006 [astro-ph.HE]].
[5] K. N. Abazajian and M. Kaplinghat, Phys. Rev. D **86**, 083511 (2012) [arXiv:1207.6047 [astro-ph.HE]].
[6] C. Gordon and O. Macias, Phys. Rev. D **88**, 083521 (2013) [arXiv:1306.5725 [astro-ph.HE]].
[7] D. Hooper and T. R. Slatyer, Phys. Dark Univ. **2**, 118 (2013) doi:10.1016/j.dark.2013.06.003 [arXiv:1302.6589 [astro-ph.HE]].
[8] W. C. Huang, A. Urbano and W. Xue, arXiv:1307.6862 [hep-ph].
[9] K. N. Abazajian, N. Canac, S. Horiuchi and M. Kaplinghat, arXiv:1402.4090 [astro-ph.HE].

[10] T. Daylan, D. P. Finkbeiner, D. Hooper, T. Linden, S. K. N. Portillo, N. L. Rodd and T. R. Slatyer, arXiv:1402.6703 [astro-ph.HE].
[11] F. Calore, I. Cholis and C. Weniger, arXiv:1409.0042 [astro-ph.CO].
[12] M. Ajello *et al.* [Fermi-LAT Collaboration], arXiv:1511.02938 [astro-ph.HE].
[13] A. Geringer-Sameth, M. G. Walker, S. M. Koushiappas, S. E. Koposov, V. Belokurov, G. Torrealba and N. W. Evans, arXiv:1503.02320 [astro-ph.HE].
[14] T. Lacroix, C. Boehm and J. Silk, Phys. Rev. D **90**, no. 4, 043508 (2014) [arXiv:1403.1987 [astro-ph.HE]].
[15] A. Alves, S. Profumo, F. S. Queiroz and W. Shepherd, Phys. Rev. D **90**, no. 11, 115003 (2014) [arXiv:1403.5027 [hep-ph]].
[16] A. Berlin, D. Hooper and S. D. McDermott, Phys. Rev. D **89**, no. 11, 115022 (2014) [arXiv:1404.0022 [hep-ph]].
[17] P. Agrawal, B. Batell, D. Hooper and T. Lin, Phys. Rev. D **90**, no. 6, 063512 (2014) [arXiv:1404.1373 [hep-ph]].
[18] E. Izaguirre, G. Krnjaic and B. Shuve, Phys. Rev. D **90**, no. 5, 055002 (2014) [arXiv:1404.2018 [hep-ph]].
[19] D. G. Cerdeo, M. Peir and S. Robles, JCAP **1408**, 005 (2014) [arXiv:1404.2572 [hep-ph]].
[20] S. Ipek, D. McKeen and A. E. Nelson, Phys. Rev. D **90**, no. 5, 055021 (2014) [arXiv:1404.3716 [hep-ph]].
[21] P. Ko, W. I. Park and Y. Tang, JCAP **1409**, 013 (2014) [arXiv:1404.5257 [hep-ph]].
[22] C. Boehm, M. J. Dolan and C. McCabe, Phys. Rev. D **90**, no. 2, 023531 (2014) [arXiv:1404.4977 [hep-ph]].
[23] M. Abdullah, A. DiFranzo, A. Rajaraman, T. M. P. Tait, P. Tanedo and A. M. Wijangco, Phys. Rev. D **90**, no. 3, 035004 (2014) [arXiv:1404.6528 [hep-ph]].
[24] D. K. Ghosh, S. Mondal and I. Saha, JCAP **1502**, no. 02, 035 (2015) [arXiv:1405.0206 [hep-ph]].
[25] A. Martin, J. Shelton and J. Unwin, Phys. Rev. D **90**, no. 10, 103513 (2014) [arXiv:1405.0272 [hep-ph]].
[26] A. Berlin, P. Gratia, D. Hooper and S. D. McDermott, Phys. Rev. D **90**, no. 1, 015032 (2014) [arXiv:1405.5204 [hep-ph]].
[27] T. Basak and T. Mondal, arXiv:1405.4877 [hep-ph].
[28] J. M. Cline, G. Dupuis, Z. Liu and W. Xue, JHEP **1408**, 131 (2014) [arXiv:1405.7691 [hep-ph]].
[29] T. Han, Z. Liu and S. Su, JHEP **1408**, 093 (2014) [arXiv:1406.1181 [hep-ph]].
[30] W. Detmold, M. McCullough and A. Pochinsky, Phys. Rev. D **90**, no. 11, 115013 (2014) [arXiv:1406.2276 [hep-ph]].
[31] L. Wang and X. F. Han, Phys. Lett. B **739**, 416 (2014) [arXiv:1406.3598 [hep-ph]].
[32] W. F. Chang and J. N. Ng, Phys. Rev. D **90**, no. 6, 065034 (2014) [arXiv:1406.4601 [hep-ph]].
[33] C. Arina, E. Del Nobile and P. Panci, Phys. Rev. Lett. **114**, 011301 (2015) [arXiv:1406.5542 [hep-ph]].
[34] C. Cheung, M. Papucci, D. Sanford, N. R. Shah and K. M. Zurek, Phys. Rev. D **90**, no. 7, 075011 (2014) [arXiv:1406.6372 [hep-ph]].
[35] J. Huang, T. Liu, L. T. Wang and F. Yu, Phys. Rev. D **90**, no. 11, 115006 (2014) [arXiv:1407.0038 [hep-ph]].
[36] C. Balzs and T. Li, Phys. Rev. D **90**, no. 5, 055026 (2014) [arXiv:1407.0174 [hep-ph]].
[37] P. Ko and Y. Tang, JCAP **1501**, 023 (2015) [arXiv:1407.5492 [hep-ph]].

[38] S. Baek, P. Ko and W. I. Park, arXiv:1407.6588 [hep-ph].
[39] N. Okada and O. Seto, Phys. Rev. D **90**, no. 8, 083523 (2014) [arXiv:1408.2583 [hep-ph]].
[40] N. F. Bell, S. Horiuchi and I. M. Shoemaker, Phys. Rev. D **91**, no. 2, 023505 (2015) [arXiv:1408.5142 [hep-ph]]; E. Hardy, R. Lasenby and J. Unwin, JHEP **1407**, 049 (2014) [arXiv:1402.4500 [hep-ph]].
[41] A. D. Banik and D. Majumdar, Phys. Lett. B **743**, 420 (2015) [arXiv:1408.5795 [hep-ph]].
[42] D. Borah and A. Dasgupta, Phys. Lett. B **741**, 103 (2015) [arXiv:1409.1406 [hep-ph]].
[43] M. Cahill-Rowley, J. Gainer, J. Hewett and T. Rizzo, JHEP **1502**, 057 (2015) [arXiv:1409.1573 [hep-ph]].
[44] J. H. Yu, Phys. Rev. D **90**, no. 9, 095010 (2014) [arXiv:1409.3227 [hep-ph]].
[45] J. Guo, J. Li, T. Li and A. G. Williams, arXiv:1409.7864 [hep-ph].
[46] J. Cao, L. Shang, P. Wu, J. M. Yang and Y. Zhang, Phys. Rev. D **91**, no. 5, 055005 (2015) [arXiv:1410.3239 [hep-ph]].
[47] Z. H. Yu, X. J. Bi, Q. S. Yan and P. F. Yin, Phys. Rev. D **91**, no. 3, 035008 (2015) [arXiv:1410.3347 [hep-ph]].
[48] M. Freytsis, D. J. Robinson and Y. Tsai, Phys. Rev. D **91**, no. 3, 035028 (2015) [arXiv:1410.3818 [hep-ph]].
[49] M. Heikinheimo and C. Spethmann, JHEP **1412**, 084 (2014) [arXiv:1410.4842 [hep-ph]].
[50] P. Agrawal, B. Batell, P. J. Fox and R. Harnik, arXiv:1411.2592 [hep-ph].
[51] K. Cheung, W. C. Huang and Y. L. S. Tsai, arXiv:1411.2619 [hep-ph].
[52] G. Arcadi, Y. Mambrini and F. Richard, JCAP **1503**, no. 03, 018 (2015) [arXiv:1411.2985 [hep-ph]].
[53] D. Hooper, Phys. Rev. D **91**, no. 3, 035025 (2015) [arXiv:1411.4079 [hep-ph]].
[54] Q. Yuan and K. Ioka, arXiv:1411.4363 [astro-ph.HE].
[55] F. Calore, I. Cholis, C. McCabe and C. Weniger, Phys. Rev. D **91**, no. 6, 063003 (2015) [arXiv:1411.4647 [hep-ph]].
[56] J. Liu, N. Weiner and W. Xue, arXiv:1412.1485 [hep-ph].
[57] A. Biswas, arXiv:1412.1663 [hep-ph].
[58] K. Ghorbani and H. Ghorbani, arXiv:1501.00206 [hep-ph]; K. Ghorbani and H. Ghorbani, arXiv:1504.03610 [hep-ph].
[59] D. G. Cerdeno, M. Peiro and S. Robles, arXiv:1501.01296 [hep-ph].
[60] A. Biswas, D. Majumdar and P. Roy, arXiv:1501.02666 [hep-ph].
[61] A. Alves, A. Berlin, S. Profumo and F. S. Queiroz, arXiv:1501.03490 [hep-ph].
[62] M. Kaplinghat, T. Linden and H. B. Yu, arXiv:1501.03507 [hep-ph].
[63] A. Berlin, A. DiFranzo and D. Hooper, arXiv:1501.03496 [hep-ph].
[64] C. H. Chen and T. Nomura, arXiv:1501.07413 [hep-ph].
[65] J. Guo, Z. Kang, P. Ko and Y. Orikasa, arXiv:1502.00508 [hep-ph].
[66] M. R. Buckley, E. Charles, J. M. Gaskins, A. M. Brooks, A. Drlica-Wagner, P. Martin and G. Zhao, [arXiv:1502.01020 [astro-ph.HE]].
[67] K. P. Modak and D. Majumdar, arXiv:1502.05682 [hep-ph].
[68] A. Achterberg, S. Caron, L. Hendriks, R. Ruiz de Austri and C. Weniger, arXiv:1502.05703 [hep-ph].
[69] T. Gherghetta, B. von Harling, A. D. Medina, M. A. Schmidt and T. Trott, arXiv:1502.07173 [hep-ph].
[70] G. Elor, N. L. Rodd and T. R. Slatyer, arXiv:1503.01773 [hep-ph].
[71] J. Kopp, J. Liu and X. P. Wang, arXiv:1503.02669 [hep-ph].

[72] X. J. Bi, L. Bian, W. Huang, J. Shu and P. F. Yin, arXiv:1503.03749 [hep-ph].
[73] T. Appelquist, R. C. Brower, M. I. Buchoff, G. T. Fleming, X. Y. Jin, J. Kiskis, G. D. Kribs and E. T. Neil *et al.*, arXiv:1503.04203 [hep-ph].
[74] A. Rajaraman, J. Smolinsky and P. Tanedo, arXiv:1503.05919 [hep-ph].
[75] J. M. Cline, G. Dupuis, Z. Liu and W. Xue, arXiv:1503.08213 [hep-ph].
[76] K. Kong and J. C. Park, Nucl. Phys. B **888**, 154 (2014) [arXiv:1404.3741 [hep-ph]].
[77] T. Bringmann, M. Vollmann and C. Weniger, Phys. Rev. D **90**, no. 12, 123001 (2014) [arXiv:1406.6027 [astro-ph.HE]].
[78] M. Cirelli, D. Gaggero, G. Giesen, M. Taoso and A. Urbano, JCAP **1412**, no. 12, 045 (2014) [arXiv:1407.2173 [hep-ph]].
[79] I. Cholis, D. Hooper and T. Linden, arXiv:1408.6224 [astro-ph.HE].
[80] Q. Yuan and B. Zhang, JHEAp **3-4**, 1 (2014) [arXiv:1404.2318 [astro-ph.HE]].
[81] E. Carlson and S. Profumo, Phys. Rev. D **90**, no. 2, 023015 (2014) [arXiv:1405.7685 [astro-ph.HE]].
[82] J. Petrovic, P. D. Serpico and G. Zaharijas, JCAP **1410**, no. 10, 052 (2014) [arXiv:1405.7928 [astro-ph.HE]].
[83] B. D. Fields, S. L. Shapiro and J. Shelton, Phys. Rev. Lett. **113**, 151302 (2014) [arXiv:1406.4856 [astro-ph.HE]].
[84] I. Cholis, D. Hooper and T. Linden, arXiv:1407.5625 [astro-ph.HE].
[85] B. Zhou, Y. F. Liang, X. Huang, X. Li, Y. Z. Fan, L. Feng and J. Chang, arXiv:1406.6948 [astro-ph.HE].
[86] C. Gordon and O. Macias, arXiv:1410.7840 [astro-ph.HE].
[87] R. M. O'Leary, M. D. Kistler, M. Kerr and J. Dexter, arXiv:1504.02477 [astro-ph.HE].
[88] J. Petrovi, P. D. Serpico and G. Zaharijas, JCAP **1502**, no. 02, 023 (2015) [arXiv:1411.2980 [astro-ph.HE]].
[89] R. Bartels, S. Krishnamurthy and C. Weniger, arXiv:1506.05104 [astro-ph.HE].
[90] S. K. Lee, M. Lisanti, B. R. Safdi, T. R. Slatyer and W. Xue, arXiv:1506.05124 [astro-ph.HE].
[91] M. Ackermann *et al.* [Fermi-LAT Collaboration], Phys. Rev. Lett. **115**, no. 23, 231301 (2015) doi:10.1103/PhysRevLett.115.231301 [arXiv:1503.02641 [astro-ph.HE]].
[92] S. Baek, P. Ko, W. I. Park and Y. Tang, JCAP **1406**, 046 (2014) [arXiv:1402.2115 [hep-ph]].
[93] T. Sjostrand, S. Mrenna and P. Z. Skands, JHEP **0605**, 026 (2006) [hep-ph/0603175].
[94] J. F. Navarro, C. S. Frenk and S. D. M. White, Astrophys. J. **462**, 563 (1996) [astro-ph/9508025].
[95] S. Baek, P. Ko and W. I. Park, JHEP **1202**, 047 (2012) [arXiv:1112.1847 [hep-ph]].
[96] S. Baek, P. Ko, W. I. Park and E. Senaha, JHEP **1211**, 116 (2012) [arXiv:1209.4163 [hep-ph]].
[97] S. Baek, P. Ko, W. I. Park and E. Senaha, JHEP **1305**, 036 (2013) [arXiv:1212.2131 [hep-ph]].
[98] S. Baek, P. Ko and W. I. Park, JHEP **1307**, 013 (2013) [arXiv:1303.4280 [hep-ph]].
[99] S. Baek, P. Ko and W. I. Park, JCAP **1410**, no. 10, 067 (2014) [arXiv:1311.1035 [hep-ph]].
[100] P. Ko and Y. Tang, JCAP **1405**, 047 (2014) [arXiv:1402.6449 [hep-ph], arXiv:1402.6449].
[101] P. Ko and Y. Tang, Phys. Lett. B **739**, 62 (2014) [arXiv:1404.0236 [hep-ph]].
[102] S. Baek, P. Ko and W. I. Park, Phys. Rev. D **90**, no. 5, 055014 (2014) [arXiv:1405.3530 [hep-ph]].
[103] V. V. Khoze and G. Ro, JHEP **1410**, 61 (2014) [arXiv:1406.2291 [hep-ph]].
[104] K. Cheung, P. Ko, J. S. Lee and P. Y. Tseng, arXiv:1507.06158 [hep-ph].
[105] **CMS** , C. Collaboration, *A combination of searches for the invisible decays of the Higgs boson using the CMS detector*, .

[106] D. S. Akerib *et al.* [LUX Collaboration], Phys. Rev. Lett. **112**, 091303 (2014) [arXiv:1310.8214 [astro-ph.CO]].